of the π-bonding component of the metal–metal bond.

The tertiary phosphine–isocyanide complexes of the types $[Mo(CNR)_6(PR_3)]^{2+}$ and $[Mo(CNR)_5(PR_3)_2]^{2+}$ are electronically related to the mixed halide–isocyanides $[Mo(CNR)_6X]^+$ and $[Mo(CNR)_5X_2]$ which have previously been isolated by Lippard and co-workers[3] and Bonati and Minghetti.[23] While the latter halogen-containing species have been used as intermediates[3,11] on the way to homoleptic $[Mo(CNR)_7]^{2+}$, our discovery that the $[Mo(CNR)_7]^{2+}$ cations react with phosphine to give mixed-ligand species points to the existence of an extensive substitution chemistry for $[Mo(CNR)_7]^{2+}$ in their reactions with neutral donors.[24] This is of particular significance bearing in mind the formal "isoelectronic" relationship between $[Mo(CNR)_7]^{2+}$, $Mo(CNAr)_6$ (Ar = aryl), and $Mo(CO)_6$; i.e., all are 18-electron systems.

With the current interest in the structures of seven-coordinate isocyanide complexes of molybdenum(II) and tungsten(II)[2-4,25-27] and the need to assess those factors which favor one geometry over another (capped trigonal prism,[3,4,25] capped octahedron,[2] and 4:3 piano stool[26]) our isolation of four different groups of mixed-ligand complexes, viz., $[Mo(CNR)_5(dppm)]^{2+}$, $[Mo(CNR)_5(dppe)]^{2+}$, $[Mo(CNR)_5(PR_3)_2]^{2+}$, and $[Mo(CNR)_6(PR_3)]^{2+}$, provides an excellent opportunity to pursue further the structures of such complexes. Accordingly, we plan to carry out single-crystal X-ray structure determinations on representatives of these groups in the very near future.

Acknowledgment. This work was supported by the National Science Foundation (Grant CHE-79-09233). We thank Professors Stephen J. Lippard and Joe San Filippo, Jr., for informing us of the status of their studies dealing with isocyanide complexes of molybdenum(II) and tungsten(II). The assistance of Professor J. B. Grutzner and Ms. E. M. Rather in obtaining the ^{31}P NMR spectra is appreciated.

Registry No. $[Mo(CNCH_3)_5(dppm)](PF_6)_2$, 74081-65-5; $[Mo(CNC(CH_3)_3)_5(dppm)](PF_6)_2$, 74096-43-8; $[Mo(CNC_6H_{11})_5(dppm)](PF_6)_2$, 74096-45-0; $[Mo(CNCH_3)_5(dppe)](PF_6)_2$, 74096-47-2; $[Mo(CNC(CH_3)_3)_5(dppe)](PF_6)_2$, 74096-49-4; $[Mo(CNC_6H_{11})_5(dppe)](PF_6)_2$, 74096-51-8; $[Mo(CNCH_3)_5(P(C_3H_7)_3)_2](PF_6)_2$, 74081-67-7; $[Mo(CNCH_3)_5(P(C_4H_9)_3)_2](PF_6)_2$, 74096-53-0; $[Mo(CNC_6H_{11})_5(P(C_2H_5)_3)_2](PF_6)_2$, 74096-55-2; $[Mo(CNC_6H_{11})_5(P(C_6H_5)_3C_2H_5)_2](PF_6)_2$, 74096-57-4; $[Mo(CNCH_3)_6(P(C_2H_5)_3)](PF_6)_2$, 74096-59-6; $[Mo(CNC(CH_3)_3)_6(P(C_2H_5)_3)](PF_6)_2$, 74096-61-0; $[Mo(CNC(CH_3)_3)_6(P(C_3H_7)_3)](PF_6)_2$, 74096-63-2; $[Mo(CNCH_3)_7](PF_6)_2$, 66632-84-6; $[Mo(CNC_6H_{11})_7](PF_6)_2$, 72155-82-9; $[Mo(CNC(CH_3)_3)_7](PF_6)_2$, 41982-05-2; $Mo_2Cl_4(dppm)_2$, 64508-35-6; α-$Mo_2Cl_4(dppe)_2$, 64490-77-3; $Mo_2Cl_4(P(C_2H_5)_3)_4$, 59780-36-8; $Mo_2Cl_4(PEtPh_2)_4$, 59752-92-0; $Mo_2Cl_4(P(n\text{-}Pr)_3)_4$, 59780-37-9.

(23) Bonati, F.; Minghetti, G. *Inorg. Chem.* **1970**, *9*, 2642.
(24) Substitution reactions of the type $[Mo(CNR)_7]^{2+} + X^- \rightleftharpoons [Mo(CNR)_6X]^+ + RNC$, where X = Cl, Br, or I, have been investigated (see: Lippard, S. J. *Prog. Inorg. Chem.* **1976**, *21*, 91).
(25) Lewis, D. F.; Lippard, S. J. *Inorg. Chem.* **1972**, *11*, 621.
(26) Dreyer, E. B.; Lam, C. T.; Lippard, S. J. *Inorg. Chem.* **1979**, *18*, 1904.
(27) LaRue, W. A.; Liu, A. T.; San Filippo, J., Jr. *Inorg. Chem.* **1980**, *19*, 315.

Contribution from the Department of Chemistry, Brown University, Providence, Rhode Island 02912

Complexes of d^8 Metals with Tetrathiomolybdate and Tetrathiotungstate Ions. Synthesis, Spectroscopy, and Electrochemistry[1]

KENNETH P. CALLAHAN* and PAMELA A. PILIERO

Received January 18, 1980

The synthesis of $Pd(MoS_4)_2^{2-}$, $Pd(WS_4)_2^{2-}$, and $Pt(MoS_4)_2^{2-}$ has been achieved, and improved methods for the Ni analogues and $Pt(WS_4)_2^{2-}$ have been developed. Infrared spectra of these compounds reflect the effects of changing the central d^8 metal. These complexes undergo reversible electrochemical reductions (Ni, Pd) quite sensitive to the nature of the d^8 metal but less so to the ligand. Two well-separated one-electron reversible reductions are seen for the nickel complexes. These move closer together in the Pd species and the second reduction becomes irreversible. Only one reduction wave is observed for the Pt complexes, but it appears to be an overlap of two different electrode processes. The electrochemical results are consistent with a decreased separation of the a_g and b_{1g} orbitals as the mass of the central metal increases. All compounds show irreversible, multielectron oxidations, probably localized on the terminal sulfur atoms of the ligands.

Introduction

Complexes of bidentate sulfur ligands with transition metals having d^8 electronic configurations have been of continuing interest for nearly 20 years.[2,3] Only recently, however, have the disputes as to the nature of the redox processes which some of these species exhibit been apparently resolved.[4,5] An example of this situation is $Ni(mnt)_2^z$, where mnt is the maleonitriledithiolate ion and z ranges from 0 to 3–; it now seems established that the sequential reductions of the neutral complex occur both on the ligand and at the metal, the exact location being a function of the particular one-electron redox couple.[5] We have studied a series of complexes in which the bidentate sulfur ligand also possesses a potentially electroactive metal and report the details of this system. A preliminary account has already appeared.[6]

Synthesis

Müller[7-9] originally reported the preparation of $Ni(MoS_4)_2^{2-}$, $Ni(WS_4)_2^{2-}$, and later $Pt(WS_4)_2^{2-}$. We have extended this

* To whom correspondence should be addressed at Occidental Research Corp., P.O. Box 19601, Irvine, CA 92713.
(1) Taken in part from the dissertation of P. A. Piliero, Brown University, 1978; presented in part at the 174th National Meeting of the American Chemical Society, Chicago, Ill., Aug 1977.
(2) R. Eisenberg, *Prog. Inorg. Chem.*, **12**, 295 (1970).
(3) J. McCleverty, *Prog. Inorg. Chem.*, **10**, 49 (1968).
(4) W. E. Geiger, Jr., T. E. Mines, and F. C. Senftleber, *Inorg. Chem.*, **14**, 2141 (1975).
(5) F. C. Senftleber and W. E. Geiger, Jr., *J. Am. Chem. Soc.*, **97**, 5018 (1975); W. E. Geiger, Jr., C. S. Allen, T. E. Mines, and F. C. Senftleber, *Inorg. Chem.*, **16**, 2003 (1977).
(6) K. P. Callahan and P. A. Piliero, *J. Chem. Soc., Chem. Commun.*, 13 (1979).
(7) A. Müller and E. Diemann, *J. Chem. Soc. D*, 65 (1971).
(8) A. Müller, E. Diemann, and H.-H. Heinsen, *Chem. Ber.*, **104**, 975 (1971).
(9) A. Müller, M. C. Chakravorti, and H. Dornfeld, *Z. Naturforsch. B: Anorg. Chem., Org. Chem.*, **30B**, 162 (1975).

0020-1669/80/1319-2619$01.00/0

Table I. Significant Infrared Absorption Frequencies (cm^{-1}) of $M(M'S_4)_2^{2-}$ Complexes[a]

compd	$(M'=S)_t$	$(M'-S)_{br}$	M–S	bending modes
$(Pr_4N)_2Ni(MoS_4)_2$	509, 494	456, 445	330, 328	220, 185, 178, 135
$(Ph_4P)_2Ni(MoS_4)_2$	512, 499	455, 443	327, 324	222, 184, 178, 169
$(Pr_4N)_2Pd(MoS_4)_2$	510, 496	451, 436	312, 295	203, 185, 173
$(Ph_4P)_2Pd(MoS_4)_2$	513, 497	450, 435	312, 295	205, 183, 173, 169
$(Pr_4N)_2Pt(MoS_4)_2$	513, 497	459, 436	345, 330, 310	195, 183, 169
$(Ph_4P)_2Pt(MoS_4)_2$	510, 496	454, 433	327, 309	198, 183, 170, 166
$(Et_4N)_2Ni(WS_4)_2$	499, 491	448	328, 320	202, 185, 180, 170
$(Ph_4P)_2Ni(WS_4)_2$	498, 496	448	328, 322	204, 180, 172, 164
$(Et_4N)_2Pd(WS_4)_2$	502, 492	439	307, 291	189, 171, 163, 157
$(Ph_4P)_2Pd(WS_4)_2$	499, 491	440	312, 295	190, 170, 164, 152
$(Et_4N)_2Pt(WS_4)_2$	500, 495	447, 440	348, 303, 268	188, 170, 161, 153
$(Ph_4P)_2Pt(WS_4)_2$	498, 491	447, 438	328, 310(sh)[b]	189, 168, 160, 147

[a] Assignments according to Cormier.[14] [b] sh = shoulder.

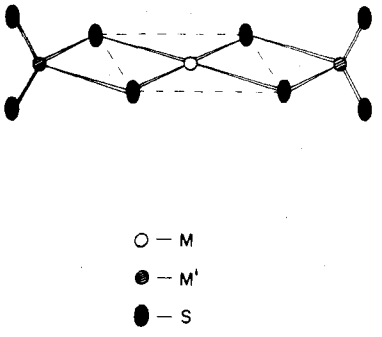

Figure 1. Schematic structure of $[M(M'S_4)_2]^{2-}$ complexes: M = Ni(II), Pd(II), Pt(II); M' = Mo(VI), W(VI).

work by preparing the Pd complexes of MoS_4^{2-} and WS_4^{2-} as well as $Pt(MoS_4)_2^{2-}$ and in the process have developed higher yield syntheses of the previously known compounds. The main preparative modifications involve the use of mixed aqueous–polar organic solvents, rather than water alone, and choice of starting material K_2PtCl_4 for the Pt(II) compounds, rather than K_2PtI_6.[9] The products were isolated as R_4N^+ or Ph_4P^+ salts and could be readily purified by recrystallization from polar organic solvents. Details are provided in the Experimental Section.

Characterization

All new compounds were characterized by elemental analyses (see Experimental Section), while samples of previously reported compounds were compared with their literature properties, primarily UV–visible and infrared spectra. All new compounds, as well as our preparations of previously known complexes, were diamagnetic in the solid state[10] and in solution.[11] The proposed structure of all these compounds, recently confirmed for $(Ph_4P)_2Ni(MoS_4)_2$ by an X-ray study,[12] is the square-planar configuration shown in Figure 1.

Infrared Spectra

Müller and co-workers have intensively studied the infrared spectra of the complexes of MoS_4^{2-} and WS_4^{2-},[8,13-15] and isotopically enriched samples have been used to completely assign the observed spectra by normal-coordinate analyses. The IR spectra of the new compounds we have prepared are consistent with these assignments[16] and with a square-planar geometry about the central d^8 metal. Small spectral changes are observed in the M–S–M' bridge vibrations as the mass of M is increased from Ni to Pd to Pt and that of M' from Mo to W, but the shifts are less than predicted by simple reduced-mass calculations, presumably due to changes in force constants as well as mixing of several vibrational modes, as indicated by the normal-coordinate analysis.[14,15] Important observed vibrational frequencies of new complexes, or incompletely reported spectra of previously known compounds, and their assignments, are presented in Table I.[16]

Table II. Electronic Spectra[a]

compd	λ_{max}[b] (ϵ[c])
$Ni(MoS_4)_2^{2-}$	30.3, 35.6, 40.3 (sh),[e] 46.1[d]
$Ni(WS_4)_2^{2-}$	15.3, 18.7, 23.5, 26.7, 30.3, 34.5 (sh), 38.2, 40.5, 47.6[d]
$Pd(MoS_4)_2^{2-}$	21.4 (1.2), 26.3 (sh), 28.7 (1.5), 32.0 (2.4), 36.5 (sh), 37.3 (3.4)
$Pd(WS_4)_2^{2-}$	25.3 (2.1), 27.4 (2.1), 32.2 (2.1), 35.0 (sh), 39.7 (2.0), 44.4[d]
$Pt(MoS_4)_2^{2-}$	21.3 (1.2), 26.0 (sh), 28.7 (1.5), 30.8 (2.8), 36.5 (sh), 37.2 (3.4), 44.4 (10.0)
$Pt(WS_4)_2^{2-}$	25.3 (2.0), 27.5 (2.0), 32.0 (2.3), 35.0 (sh), 40.0 (3.7), 44.4[d]

[a] Et_4N^+ salts in CH_3CN solution. [b] In $cm^{-1} \times 10^{-3}$. [c] In L mol^{-1} $cm^{-1} \times 10^{-4}$. [d] Extinction coefficient(s) not determined. [e] sh = shoulder.

Electronic Spectra

The free ligands are colored (MoS_4^{2-}, red; WS_4^{2-}, yellow-orange) due to tailing of intense sulfur to metal charge-transfer bands into the visible region of the spectrum; Mo and W are in their highest oxidation states and no d–d transitions can occur. Ligand to metal charge-transfer bands also appear to dominate the spectra of the d^8 metal complexes of these ions; these transitions extend into the spectral regions where d–d transitions of the d^8 metals are expected to appear, so little or no information about the electronic strcutures of these compounds can be obtained from their electronic spectra. The observed absorption maxima and extinction coefficients are presented in Table II.

Electrochemistry

The similarity of the metal tetrathiomolybdates or -tungstates to the well-known metal dithiolenes[2,3] and dithiocarbamates,[17] both of which exhibit extensive and often reversible redox behavior, led us to examine the electrochemical behavior of these compounds. Cyclic voltammetry at a platinum-button electrode was employed, for the compounds

(10) We thank Drs. C. Derrington and D. Schleich and Professor A. Wold for these measurements.
(11) Sharp, completely resolved ^1H NMR signals of cations and solvent were observed for these compounds.
(12) I. Søtofte, *Acta Chem. Scand., Ser. A*, **A30**, 157 (1976).
(13) A. Müller, E. Ahlborn, and H.-H. Heinsen, *Z. Anorg. Allg. Chem.*, **386**, 102 (1971).
(14) A. Cormier, K. Nakamoto, E. Ahlborn, and A. Müller, *J. Mol. Struct.*, **25**, 43 (1975).
(15) E. Koniger-Ahlborn, A. Müller, A. D. Cormier, J. D. Brown, and K. Nakamoto, *Inorg. Chem.*, **14**, 2009 (1975).
(16) The bands at 209 and 204 cm^{-1} assigned[9] as bending modes of the anion in $(Ph_4P)_2Pt(WS_4)_2$ are, in fact, vibrations of the Ph_4P^+ cation.
(17) D. Coucouvanis, *Prog. Inorg. Chem.* **11**, 233 (1970).

Table III. Electrochemical Parameters of Nickel Complexes[a]

		$Ni(MoS_4)_2^{2-}$				$Ni(WS_4)_2^{2-}$			
solvent	electrolyte	$E^\circ(1)$	i_a/i_c	$E^\circ(2)$	i_a/i_c	$E^\circ(1)$	i_a/i_c	$E^\circ(2)$	i_a/i_c
CH_3CN	Et_4NClO_4	−0.544	1.06, 0.94	−1.310	1.01, 0.96	−0.556	0.98, 1.00	−1.493	0.91, 0.94
CH_3CN	Et_4NBr	−0.530		−1.286		−0.537		−1.472	
CH_3CN	Et_4NI	−0.535		−1.301		−0.545		−1.482	
CH_3CN	Pr_4NBr	−0.554		−1.350		−0.551		−1.497	
DMF	Et_4NClO_4	−0.606	0.97, 0.94	−1.396	1.07, 1.05	−0.614	0.85, 0.91	−1.573	0.90, 0.87

[a] E° values in volts vs. SCE; $E^\circ = (E_c + E_a/2)$; i_a/i_c values observed at 1.2 and 6 V min^{-1} scan rates.

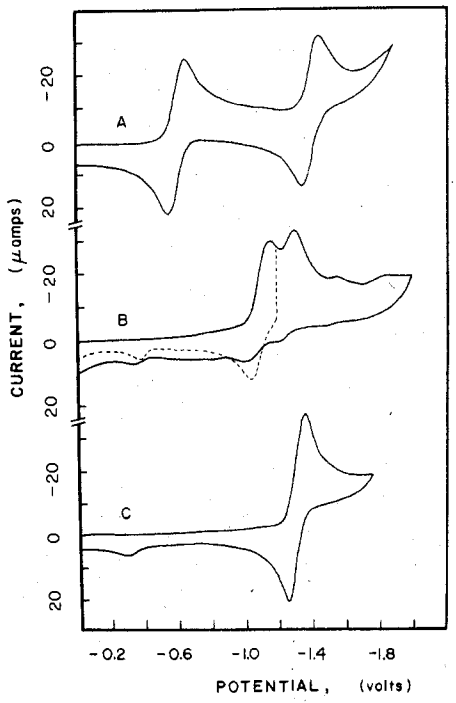

Figure 2. Cyclic voltammograms of (A) $(Pr_4N)_2Ni(MoS_4)_2$, (B) $(Et_4N)_2Pd(MoS_4)_2$, and (C) $(Et_4N)_2Pt(MoS_4)_2$ in DMF–Et_4NClO_4; scan rate 3 V min^{-1}; potentials vs. SCE.

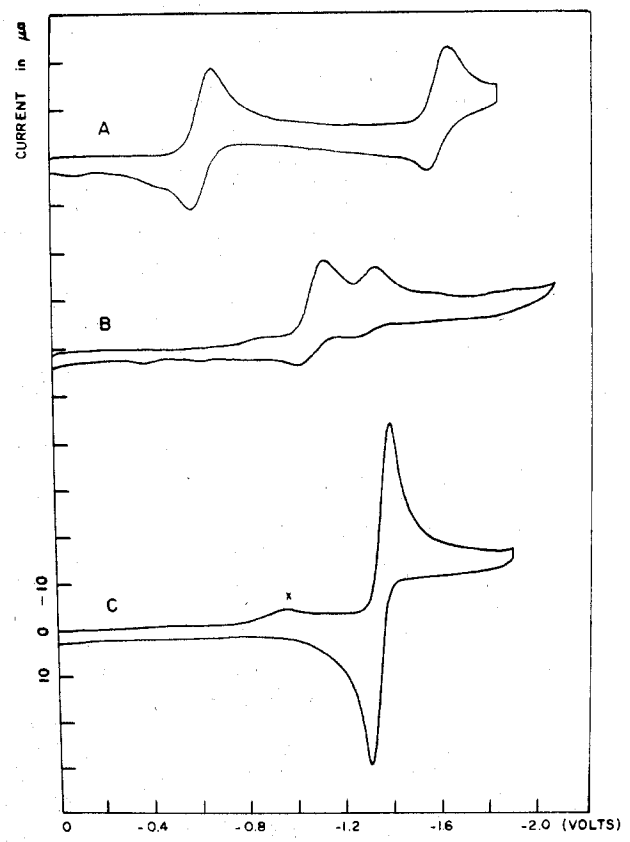

Figure 3. Cyclic voltammograms of (A) $(Pr_4N)_2Ni(WS_4)_2$, (B) $(Et_4N)_2Pd(WS_4)_2$, and (C) $(Et_4N)_2Pt(WS_4)_2$ in DMF–Et_4NClO_4 (× = impurity); scan rate 1.2 V min^{-1}; potentials held 30 s before scan reversal in parts A and C; potentials vs. SCE.

were found to react with mercury. Experiments were carried out in both acetonitrile and *N,N'*-dimethylformamide (DMF) solutions, and with several different supporting electrolytes, to test medium effects on the electrode processes. Detailed descriptions of the results are presented in the following sections.

A. Reductions. Representative cyclic voltammograms of the reductions shown by the $M(MoS_4)_2^{2-}$ and $M(WS_4)_2^{2-}$ complexes are presented in Figures 2 and 3, respectively. As the nature of the reductions is primarily dependent on the central metal, the Ni, Pd, and Pt compounds are discussed in turn. The free $M'S_4^{2-}$ ligands exhibited substantially different behavior than their complexes, undergoing broad, multistep, irreversible reductions at potentials between −0.8 and −1.4 V.

1. Nickel Complexes. Both $Ni(MoS_4)_2^{2-}$ and $Ni(WS_4)_2^{2-}$ exhibited two isolated and sequential reversible one-electron reductions. The first and second reduction potentials were separated by 0.8 V in the former complex and by 0.95 V in the latter. The first reduction potentials of the two complexes were nearly identical, but the second reduction potential of $Ni(WS_4)_2^{2-}$ was roughly 150 mV more negative than the corresponding wave of $Ni(MoS_4)_2^{2-}$.

Typical cyclic voltammograms of the nickel complexes of MoS_4^{2-} and WS_4^{2-} in DMF with 0.1 M Et_4NClO_4 supporting electrolyte are shown in Figures 2A and 3A, respectively. The electrochemical behavior of these compounds was also studied in acetonitrile with 0.1 M Et_4NClO_4, Et_4NBr, Et_4NI, and Pr_4NBr supporting electrolytes. Slight differences in the potentials of the two reductions were observed when the solvent–electrolyte systems were altered. Both reductions occurred at more negative potentials in DMF than in CH_3CN (Et_4NClO_4 supporting electrolyte); the first reduction shifted 55 mV and the second wave was 83 mV more negative. Negative shifts were also observed in CH_3CN when the supporting electrolyte was changed from Et_4NClO_4 to Pr_4NBr; again, the second wave shifted the greater amount. Such changes in the redox potentials are known to arise from the differences in ion pairing of electroactive anions and the cations of the supporting electrolyte and from changes in solvation of the ion pairs.[18]

The reductions were characterized as being reversible one-electron transfers by the comparison of ΔE, half-peak width, and peak current values to those shown by ferrocene under identical conditions.[19] Pertinent numerical values are presented in Table III. The characteristics of the two nickel

(18) D. T. Sawyer and J. L. Roberts, Jr., "Experimental Electrochemistry for Chemists", Wiley, New York, 1974, pp 194–196.

(19) This method was necessary owing to a small amount of uncompensated *iR* drop in our system (since corrected) which made peak separations increase with increasing scan rate. More recent studies show that the ΔE values of the Ni and Pd reductions remain below 80 mV at scan rates up to 470 mV s^{-1}.

Table IV. Electrochemical Parameters of Palladium Complexes[a]

solvent	electrolyte	$Pd(MoS_4)_2^{2-}$ E°	$Pd(MoS_4)_2^{2-}$ E_c	$Pd(WS_4)_2^{2-}$ E°	$Pd(WS_4)_2^{2-}$ E_c
CH_3CN	Et_4NBr	−1.010	−1.175	−1.000	−1.250
CH_3CN	Pr_4NBr	−1.029	−1.340	−1.026	−1.395
DMF	Et_4NClO_4	−1.073	−1.270	−1.066	−1.310
DMF	Pr_4NBr	−1.087	−1.326	−1.055	−1.460

[a] E values are in volts vs. SCE; $E^\circ = (E_c + E_a/2)$; E_c is the peak potential of the second reduction. All values were measured at 1.2 V min^{-1}. Sample concentration 10^{-3} M; supporting electrolyte concentration 0.1 M.

complexes were almost identical. The ΔE values and half-peak widths were comparable to those of ferrocene, being well within the experimental error of ±3 mV for the potential measurements. The cathodic peak currents were approximately two-thirds the value of the peak currents shown by ferrocene, the discrepancy presumably due to differences in diffusion coefficients. The current functions of ferrocene and the nickel complexes ($i/v^{1/2}$ vs. v) had similar slopes, indicating the same influence of uncompensated iR drop on these systems.

The peak current ratios, i_a/i_c, were found to be unity or close to it, depending on the solvent–electrolyte constitution, for both reductions. The results in CH_3CN with 0.1 M Et_4NClO_4 were particularly good, with $i_a/i_c = 1.0$ for both reductions of the two complexes. The current ratios were slightly higher in CH_3CN than in DMF; in the latter solvent they ranged between 0.90 and 1.07 for $Ni(MoS_4)_2^{2-}$ and 0.84 and 0.92 for $Ni(WS_4)_2^{2-}$, at scan rates between 1.2 and 12 V min^{-1}.

Under the experimental conditions, both reduction processes produced chemically stable species which could be reoxidized back to the original complexes upon scan reversal. The electrochemically reduced species were stable for at least 1 min, as shown by a high current ratio of the first reduction on a truncated scan. $Ni(WS_4)_2^{2-}$ could be chemically reduced with a large excess of $NaBH_4$ to afford a species which gave the cyclic voltammogram expected for the trianion, although the scan had additional features presumably arising from the reductant or its oxidation product. Attempts to measure ESR spectra of these solutions were unsuccessful; no signals were detected at room or liquid-nitrogen temperatures.

These results are consistent with two reversible one-electron reductions as described by eq 1.

$$Ni(MS_4)_2^{2-} \overset{e^-}{\rightleftharpoons} Ni(MS_4)_2^{3-} \overset{e^-}{\rightleftharpoons} Ni(MS_4)_2^{4-} \quad (M = Mo, W) \quad (1)$$

2. Palladium Complexes. Both $Pd(MoS_4)_2^{2-}$ and $Pd(WS_4)_2^{2-}$ underwent two sequential reductions, but at potentials much closer together than the analogous nickel complexes. The first reduction potentials were more negative and the second reduction potentials less negative than those of the nickel analogues.

The palladium complexes were studied in CH_3CN solution with Et_4NClO_4, Et_4NBr, and Pr_4NBr supporting electrolytes and in DMF with Et_4NClO_4 and Pr_4NBr. Pertinent numerical data are listed in Table IV, and representative cyclic voltammograms are shown in Figures 2B and 3B.

The characteristics of the cyclic voltammograms shown by these complexes depended on the potential difference between the first and second reductions and the potential at which the scan was switched. Small variations in the potential difference between the first and second reductions were, in turn, dependent on the ligand and solvent–electrolyte conditions, as observed for the nickel analogues. Under some conditions there was considerable overlap of the first and second waves; they were always separated enough to give measurable peak potential values ($E_{c_2} - E_{c_1} > 118$ mV) but overlap made peak current measurements subject to error.

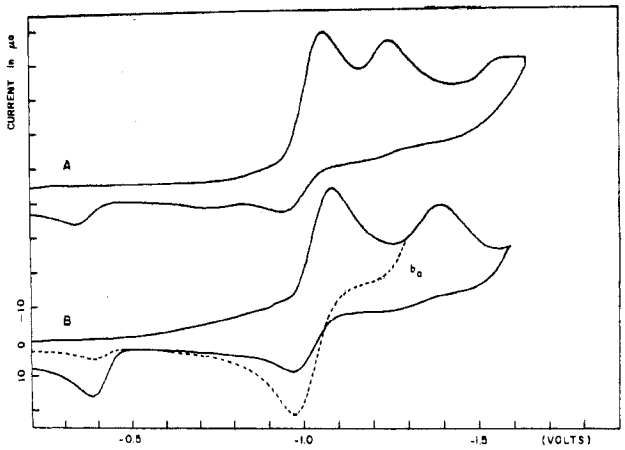

Figure 4. Cyclic voltammograms of $(Et_4N)_2Pd(WS_4)_2$ in (A) CH_3CN–Et_4NBr and (B) CH_3CN–Pr_4NBr (dashed line, $\lambda = -1.3$ V); scan rate 3 V min^{-1}; potentials vs. SCE.

Figure 4 shows cyclic voltammograms of $Pd(WS_4)_2^{2-}$ in CH_3CN with Et_4NBr and with Pr_4NBr and illustrates the medium effect observed. The reduction processes were spread further apart with Pr_4NBr supporting electrolyte. The cathodic peak currents of the first reductions were also slightly less in Pr_4NBr, where the reductions were not as close together, than in Et_4NBr.

Anodic base lines of the first reduction were difficult to measure in most of the cyclic voltammograms of the palladium complexes. Three different methods of measuring anodic base lines were employed, all with the scan reversed before the second reduction. The values of current ratios for a particular system calculated by the different methods were not always consistent, however, as the peak current values were subject to errors from wave overlap. The current ratios closest to unity were obtained when the first and second reductions had the greatest separation, as expected. Figure 4B shows that a peak separation of 315 mV allowed an anodic base line (b_a, dashed line) to be drawn for the reverse scan. In this case the measured current ratio was 1.0, with a cathodic peak current of 30 μA. The potential-hold[20] and Nicholson[21] methods were also used to determine current ratios, but the results were dependent on the methods of calculation; the value obtained by using the potential-hold method was 0.80, while that from the Nicholson method was 1.02.

The current ratios shown by $Pd(MoS_4)_2^{2-}$ were less than those of the corresponding tungstate. The former compound gave a current ratio of 0.60 in CH_3CN with 0.1 M Pr_4NBr and 0.6–0.7 in DMF with Et_4NClO_4. Current ratios of 0.3 or less were observed for the first reduction when the scan was reversed after the second reduction.

The reversibilities of the reductions of the palladium complexes were determined by current ratio values and by comparison of the ΔE, half-peak width, and cathodic peak current values to those shown by the analogous nickel complexes under similar conditions. The first reduction of $Pd(WS_4)_2^{2-}$ appeared to be a truly reversible one-electron transfer only when the scan was reversed well before onset of the second reduction and when the first and second reductions were separated by more than 300 mV, as in CH_3CN and DMF solutions with Pr_4NBr supporting electrolyte. The first reduction of the palladium thiomolybdate appeared to be a reversible one-electron transfer with respect to ΔE, half-peak width, and cathodic peak potential when the scan was reversed before the second reduction and the reductions were well separated, but

(20) R. N. Adams, "Electrochemistry at Solid Electrodes", Marcel Dekker, New York, 1969, pp 156–158.
(21) R. S. Nicholson, *Anal. Chem.*, **38**, 1406 (1966).

the current ratios never reached unity.

The second reductions of both palladium complexes appear to be both chemically and electrochemically irreversible. The chemical irreversibility can be seen in Figures 2–4 by the virtual absence of an anodic wave corresponding to the second reduction process. The product of the second reduction is therefore unstable and either decomposed or reacted in the time between the forward and reverse scans. The anodic wave of the first reduction was also substantially decreased when the scan was reversed after the second reduction, indicating that a reaction of the product of the second reduction occurred rather than reoxidation back to the trianionic species, the product of the first reduction. It can also be seen (Figures 2 and 4) that the second reduction process produced one major electroactive species which was irreversibly oxidized at ca −0.4 V. The peak currents shown by this oxidation were very low compared to the cathodic peak currents of the first reduction on the same scan. The anodic peaks at −0.4 V were larger when slow scan rates were used or when the potential was held for a period of time beyond the second reduction, indicating that this electroactive species was formed from a slow (30–60 s) chemical reaction.

The second reduction also appeared to be an electrochemically irreversible process from the low, broad shape of the second wave as shown in Figures 2–4. Electrochemical waves which are lower and more drawn out than those of reversible one-electron transfers are indicative of slower electron transfer at the electrode surface.[22]

The palladium complexes appeared to undergo a third, irreversible reduction at ca. −1.6 V. Very broad peaks were observed for this process; its cathodic peak currents were much smaller than those of the first reduction. This step was not investigated further.

These observations on the palladium complexes are consistent with a scheme involving both electron transfer (E) and chemical reaction (C) steps shown in eq 2, where A represents

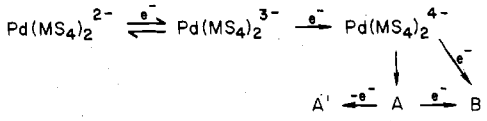

(2)

M = Mo, W

the product of a chemical reaction of the tetraanion, which is oxidized at −0.4 V to A′, and B represents the species formed at −1.6 V. The trianionic species appeared to be chemically stable under conditions when its reduction was sufficiently removed from the second reduction, as the irreversible oxidation at −0.4 V was then not observed or was at least substantially diminished.

3. Platinum Complexes. A single reduction wave was observed for the two platinum complexes. The reduction potentials were slightly more negative than the second reductions of the palladium analogues. The characteristics of these cyclic voltammograms, however, indicated that overlap of two reduction waves had occurred.

The platinum complexes were studied in the same solvent–electrolyte systems as the nickel and palladium analogues. Electrochemical data obtained for these two compounds are presented in Table V, and representative scans are shown in Figures 2C and 3C. The reduction waves showed substantial medium effects and significant departure from the behavior expected for reversible one- or two-electron reduction or an irreversible process.

(22) Reference 20, p 44. At faster scan rates, the anodic current increases but current ratios could not be accurately measured due to overlap with the first reduction. This observation is consistent with our model (eq 2).

Table V. Electrochemical Parameters of Platinum Complexes[a]

		$Pt(MoS_4)_2^{2-}$		$Pt(WS_4)_2^{2-}$	
solvent	electrolyte	E°	i_a/i_c	E°	i_a/i_c
CH_3CN	Et_4NI	−1.246	0.66		
CH_3CN	Pr_4NBr	−1.262	0.52		
CH_3CN	Et_4NClO_4			−1.293	0.67
CH_3CN	Et_4NBr			−1.270	0.73
DMF	Et_4NClO_4	−1.301	0.84	−1.346	1.02
DMF	Pr_4NBr	−1.341	0.4	−1.370	0.75

[a] Potentials in volts vs. SCE; $E^\circ = (E_c + E_a/2)$; i_a/i_c values measured at 1.2 V min^{-1} scan rate. Sample concentration 10^{-3} M; supporting electrolyte 0.1 M.

The theory of multistep electron-transfer reactions, as developed by Polcyn and Shain,[23] was used to interpret this platinum system. It was shown that a cyclic voltammogram resulting from two successive one-electron transfers, eq 3,

$$A + e^- \rightarrow B \xrightarrow{e^-} C \quad \text{(both A and B electroactive)} \quad (3)$$

would show only one wave, a composite of the two electrode processes, when the potential difference between the reductions was less than 100 mV. The characteristics of such composite waves depend upon the nature of the electron-transfer steps [reversible (R) or irreversible (I)] and the separation of the two waves. For two successive and reversible one-electron reductions (R–R), the cathodic and anodic waves of the theoretical cyclic voltammogram were symmetric but broadened and distorted at a reduction potential difference of 90 mV. The wave became taller and narrower upon closer approach of the two reductions, and at a potential difference of zero the wave showed peak current values between those of reversible one- and two-electron waves and a peak separation of 42 mV. If B is easier to reduce than A, the cyclic voltammogram resembles that of a reversible two-electron reduction, with ΔE = 30 mV, half-peak widths of 28.5 mV, and peak current 2.83 times that of a one-electron process. Situations in which one or both of the electron-transfer steps is irreversible (R–I, I–R, or I–I) could not be quantified as precisely as the R–R case, but a distorted composite wave in which the cathodic and anodic waves had dissimilar shapes was calculated.

Under different solvent–electrolyte conditions, reduction of the platinum complexes appeared to be either an R–R or an R–I or I–R process. The cyclic voltammogram of $Pt(WS_4)_2^{2-}$ in DMF with 0.1 M Et_4NClO_4 had current ratios from 1.02 to 0.97 (decreasing with increasing scan rate) and cathodic peak currents 2.25–2.58 times greater than those of $Ni(WS_4)_2^{2-}$ under identical conditions; these values suggest two nearly coincident, reversible one-electron reductions occur in this system. At a scan rate of 1.2 V min^{-1}, ΔE was found to be 42 mV and half-peak widths were 41 and 44 mV, in good agreement with the theoretical values.[23]

The cyclic voltammograms of $Pt(MoS_4)_2^{2-}$ in DMF with Et_4NClO_4 indicated less reversibility than the tungsten analogue. The current ratios varied from 0.8 to 0.9, and the half-peak width of the cathodic peak was greater than that of the anodic portion of the wave. Cathodic peak currents were 1.28–1.42 times greater than those of the one-electron reversible reductions of the nickel complexes. This behavior suggests that one of the reductions making up the composite is irreversible.

The reductions of the platinum complexes in other media were consistent with R–I or I–R situations. The most reversible behavior, with respect to current ratio, was observed in DMF with Et_4NClO_4. The processes were less reversible in CH_3CN, and use of Pr_4NBr as supporting electrolyte had a similar effect.

(23) D. S. Polcyn and I. Shain, *Anal. Chem.*, **38**, 370 (1966).

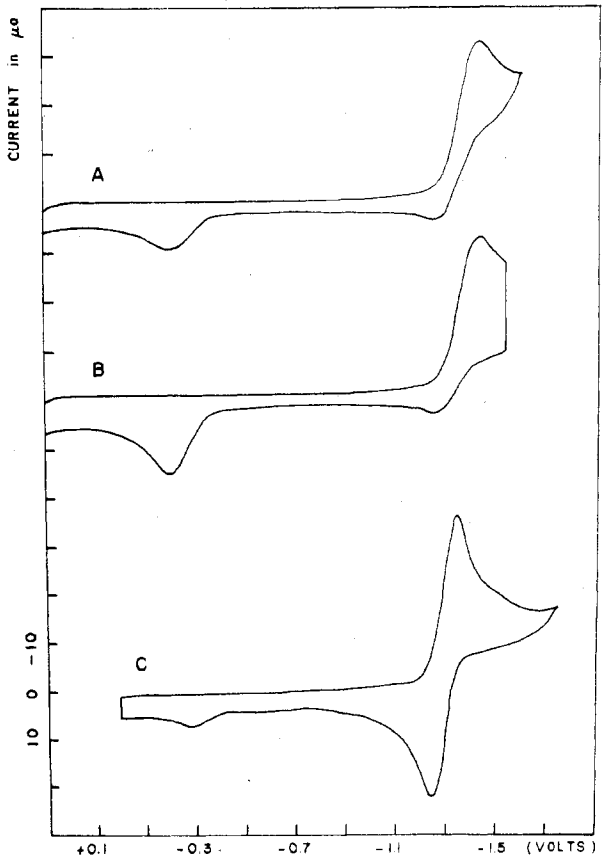

Figure 5. Cyclic voltammograms of (A) $(Ph_4P)_2Pt(MoS_4)_2$ in DMF–Pr_4NBr, (B) same as (A) with potentials held 30 s before scan reversal, and (C) $(Et_4N)_2Pt(MoS_4)_2$ in DMF–Et_4NClO_4; scan rate 3 V min^{-1}; potentials vs. SCE.

Figure 5 shows the effect of supporting electrolyte on the cyclic voltammograms of $Pt(MoS_4)_2^{2-}$. The decreased reversibility using Pr_4NBr (Figure 5A,B) rather than Et_4NClO_4 (Figure 5C) is clear. Figure 5 also shows the presence of an electroactive species which results from reaction of the reduction products; it is oxidized at ca. −0.2 V, and this oxidation current is increased when the potential is held past the reduction potential for 30 s before the reverse scan is initiated (Figure 5B). Only a small amount of this follow-up product was formed when Et_4NClO_4 was used as the supporting electrolyte (Figure 5C).

Further indications that the cyclic voltammograms of the platinum complexes were actually composite waves were two cases in which a shoulder was observed on the cathodic portion of the scan. These cases, $Pt(WS_4)_2^{2-}$ in CH_3CN with 0.1 M Et_4NBr at 3 V min^{-1} and $Pt(MoS_4)_2^{2-}$ in DMF with Et_4NClO_4 at 1.2 V min^{-1}, were the only instances, but they were reproducible. At faster scan rates the shoulders were not visible, nor could a shoulder be detected on the anodic portion of the waves.[24]

From the electrochemical data obtained on the platinum complexes, we cannot determine whether they undergo an R–I reduction process similar to that observed for the palladium analogues or an I–R sequence.

B. Oxidations. Electrochemical oxidations of MoS_4^{2-}, WS_4^{2-}, and their 2:1 complexes with Ni(II), Pd(II), and Pt(II) were also studied by cyclic voltammetry. The complexes showed behavior similar to that of their constituent ligands: broad, irreversible, multielectron oxidations at positive potentials. These systems were studied in both CH_3CN and DMF, with Et_4NClO_4 supporting electrolyte; only minor solvent effects were observed.

(24) A shoulder on the cathodic wave was recently observed for $Pt(WS_4)_2^{2-}$ in CH_3CN–Et_4NClO_4, at rapid scan rates (470 mV s^{-1}–27.7 V s^{-1}).

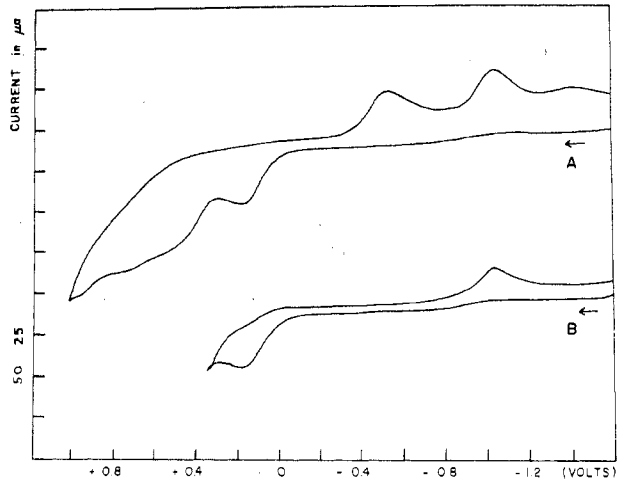

Figure 6. Cyclic voltammograms of $(Ph_4P)_2WS_4$ in DMF–Et_4NClO_4 at (A) λ = +1.02 V and (B) λ = +0.35 V; scan rate 3 V min^{-1}; arrow indicates scan direction; potentials vs. SCE.

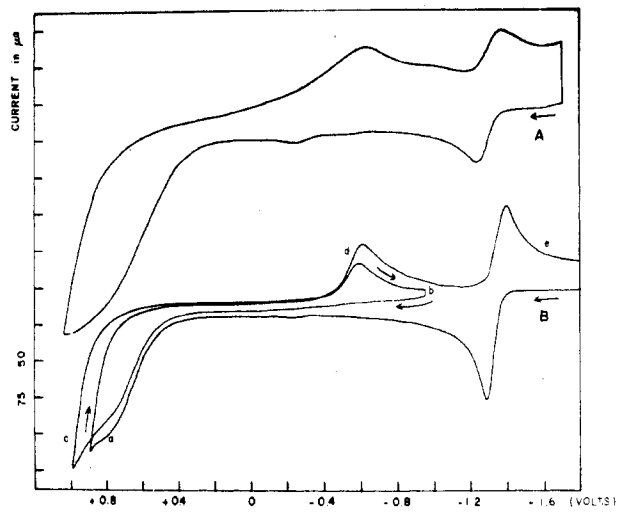

Figure 7. Cyclic voltammograms of (A) $(Et_4N)_2Pt(MoS_4)_2$, scan rate 6 V min^{-1}, and (B) $(Et_4N)_2Pt(WS_4)_2$, scan rate 3 V min^{-1}, points a → e indicating scan direction; both in DMF–Et_4NClO_4; potentials vs. SCE.

Both MoS_4^{2-} and WS_4^{2-} underwent a series of three or more poorly defined and irreversible oxidations between +0.1 and +1.0 V; the reverse scans depended on the switching potential, but the closest approach of oxidation and reduction peaks was 600 mV, more than 10 times that expected for a reversible one-electron redox couple. Typical behavior of the $M'S_4^{2-}$ ions upon oxidation is illustrated by WS_4^{2-} in Figure 6.

Oxidations of the complexes of these ions were studied by recording cyclic voltammograms starting at potentials more negative than the last reduction of the complex, e.g., at −1.7 V for $Ni(MoS_4)_2^{2-}$, and thus oxidation waves corresponding to the formation of $Ni(MoS_4)_2^{3-}$ and $Ni(MoS_4)_2^{2-}$ were observed in these scans. At more positive potentials, very broad, multielectron, irreversible oxidation waves were observed. Anodic peak currents of these oxidations were very much larger than the peak currents of the reversible reductions of these complexes, indicating the multielectron nature of these processes. Oxidations of the complexes began at more positive potentials than the oxidations of the free ligands but were similar in shape. Representative scans, those of $Pt(MoS_4)_2^{2-}$ and $Pt(WS_4)_2^{2-}$, are shown in Figure 7A,B, respectively.

Electroactive byproducts of the oxidations were observed as an irreversible reduction at ca. −0.5 V on the reverse scan if the switching potential was +1.0 V or greater. This feature can be seen in Figure 7A and was observed for all the metal complexes. The reduction wave at −1.4 V indicates that complete destruction of the complexes does not occur on oxidation, as this wave corresponds to the reduction of Pt-$(MoS_4)_2^{2-}$. The characteristic reductions of the Ni(II) and Pd(II) species could also be observed following oxidation to +1.0 V.

Figure 7B shows the irreversible nature of the −0.5 V reduction. No observable anodic peak was detected if the scan direction was switched immediately after this reduction, cycle b.

The similar behavior of the ligands and their metal complexes toward electrochemical oxidation suggests that these processes are analogous. We suggest that oxidation occurs at the terminal sulfur atoms in the complexes and that the oxidation potentials are shifted to more positive values when the free ligands are coordinated to d^8 metals.

Discussion

Synthesis of the complete set of Ni(II), Pd(II), and Pt(II) complexes of MoS_4^{2-} and WS_4^{2-} has allowed a detailed comparison of the properties of these species. The most interesting and informative results were obtained from a study of their electrochemical behavior.

We found the most surprising feature of the cyclic voltammograms of these complexes to be their dependency on the central metal while being relatively insensitive to the ligands. Only small changes are seen in the first reduction potentials of the Ni and Pd complexes when the ligands are changed from MoS_4^{2-} to WS_4^{2-}, but under similar conditions the reduction potentials of the Pd compounds are ca. 0.5 V more negative than that of their Ni analogues. This suggests that the first reductions are primarily centered at the d^8 metal, not on the ligands. This interpretation cannot be extended to the second reductions, however, for not only do these show more sensitivity to the nature of the ligand, but there is also a change from reversible to irreversible behavior in going from Ni to Pd. The unique properties of the Pt complexes underscore the complex nature of the electrochemical processes these compounds undergo.

A rough, qualitatively consistent explanation of the observed behavior can be drawn from Geiger's work on d^8 complexes of mnt, where a reordering of molecular orbitals was observed as the mass of the central metal increased. For the $M(mnt)_2^{2-} \rightarrow M(mnt)_2^{3-}$ reduction, where M was Ni or Pd, the electron entered a primarily metal-centered MO, but for M = Pt the LUMO is primarily ligand centered. We suggest that a similar situation may exist in the compounds we have studied.

In the case of the Ni complexes of MoS_4^{2-} and WS_4^{2-}, the LUMO appears to be primarily localized on the Ni, and the two reversible reductions correspond to the sequential filling of this orbital. In the case of Pd, a lessened energy difference between this metal-centered orbital, of a_g symmetry, and an orbital of predominantly ligand character having b_{1g} symmetry produces the observed reduction properties: a reversible one-electron reduction (addition of an electron to a_g) and an irreversible one-electron reduction (into b_{1g}). A process like this would occur if the separation of the a_g and b_{1g} orbitals was less than the pairing energy in a_g. Assignment of the first reduction potential to a Pd-centered orbital is validated by the insensitivity of reduction potential to the nature of the ligand; the second reduction potentials show a much greater change when the ligand is varied between MoS_4^{2-} and WS_4^{2-}.

A further decrease in the a_g–b_{1g} energy separation would lead to a situation in which they were of nearly equal energy (perhaps with b_{1g} lower in energy, as found by Geiger),[5] and reduction would involve two overlapping one-electron processes, either R–I or I–R depending on the relative energies of the two MO's. This is in agreement with our observations of the Pt compounds, although we cannot determine at this time which orbital is lowest in energy.

Although we have no rigorous support for this suggested model, we find it attractive for not only does it fit the observed behavior but also similar features have previously been established in analogous systems.[5,25] Work is in progress to test this model's validity in the present and related systems, and the results will be reported in subsequent papers.

Experimental Section

Materials. $(NH_4)_2MoS_4$ and $(NH_4)_2WS_4$ were prepared by standard procedures.[26,27] K_2PdCl_4 and K_2PtCl_4 (Matthey-Bishop, Inc.) were used as received. Reagent grade CH_3CN (Aldrich) was used for all syntheses; MCB or Aldrich Spectrograde CH_3CN was used for electrochemical measurements without further purification. *N,N'*-Dimethylformamide (DMF) was twice vacuum distilled from freshly ignited CaO before use as an electrochemical solvent; the middle 60% of the distillate was collected, and the second distillate was stored over 4-Å molecular sieves and used within 24 h. Polarographic grade $(C_2H_5)_4NClO_4$ (Southwestern Analytical Chemicals) was recrystallized twice from H_2O and dried at 70 °C in vacuo for several days. $(C_2H_5)_4NBr$ (Eastman) was recrystallized from CH_3CN and dried in vacuo. $(C_3H_7)_4NBr$ (Eastman) was recrystallized from 9:1 ethyl acetate–ethanol and dried in vacuo. Ph_4PBr (Alfa) was used as received.

Physical Measurements. Elemental analyses of new compounds were performed by Schwarzkopf Microanalytical Laboratory, Woodside, N.Y. Magnetic susceptibilities of solid samples were measured at room temperature by the Faraday method using an apparatus previously described.[28]

Infrared spectra were recorded with use of Digilab FTS-14 and FTS-15B instruments. Samples were prepared as Nujol mulls sandwiched between KBr plates for the mid-IR region (3800–400 cm^{-1}). Polyethylene plates (1.5-mm thickness) were used in the far-IR region. Very thick mulls and 1000–2000 scans were required to observe weak vibrations in the 400–50-cm^{-1} region; more dilute mulls and 100–200 scans were used in the 550–400-cm^{-1} range. Ultraviolet–visible spectra were measured on a Cary 14 spectrophotometer using 1-cm matched quartz cells. Solutions were prepared by using either Spectrograde CH_3CN or a 1:1 CH_3CN–H_2O mixture.

Electrochemical experiments were carried out by using a PAR Model 174 polarographic analyzer and a Hewlett-Packard 7045A X-Y recorder. Cyclic voltammograms were recorded at scan rates of 1.2, 3, 6, and 12 V min^{-1}. A three-electrode configuration was used for all experiments; these consisted of a saturated calomel electrode (SCE) reference similar to the design of Adams[29] connected to the solution by a salt bridge (filled with the same solvent–electrolyte combination as the sample) and a porous glass frit, a Beckman platinum-button working electrode, and a platinum-wire auxiliary electrode. The Pt electrodes were cleaned prior to each use by immersion in concentrated HNO_3 for 15 min, followed by 15 min in a saturated solution of ferrous ammonium sulfate in 1 M H_2SO_4, thorough washing in distilled water, and soaking in a stirred portion of the solvent–electrolyte solution for 10–15 min. Supporting electrolyte and sample concentrations were 0.1 and 10^{-3} M, respectively. The sample solutions were degassed with N_2 presaturated with solvent. Uncompensated *iR* drop in the system caused several parameters to deviate from their ideal values (most noticeable was the peak potential difference, ΔE); accordingly, the reversible one-electron $(C_5H_5)_2Fe \rightarrow (C_5H_5)_2Fe^+$ redox couple was used as an external reversibility standard. Cyclic voltammograms of the compounds under study were compared with those of the ferrocene system measured under identical conditions, and similar values were taken to indicate reversible behavior. Subsequent work has eliminated the *iR* drop problem and confirmed the reversible behavior reported here.

(25) R. L. Schlupp and A. H. Maki, *Inorg. Chem.*, **13**, 44 (1974).
(26) G. Kruss, *Justus Liebigs Ann. Chem.*, **225**, 6 (1884).
(27) J. J. Berzelius, *Pogg. Ann. Phys. Chem.*, **7**, 270 (1826); E. Corleis, *Justus Liebigs Ann. Chem.*, **232**, 254 (1886).
(28) B. L. Morris and A. Wold, *Rev. Sci. Instrum.*, **89**, 1937 (1968).
(29) Reference 20, pp 288–291.

Rapid-scan cyclic voltammograms were obtained by using this same equipment coupled with a Hewlett-Packard low-frequency function generator, a PAR polarographic analyzer interface, and a Tektronix Model 504 oscilloscope with Series 125 camera. Calibration was made by using a John Fluke differential voltmeter. Error in measurement of the peak potentials of fast-scan cyclic voltammograms is 20–25 mV.

Syntheses. The Ni(II), Pd(II), and Pt(II) complexes of MoS_4^{2-} and WS_4^{2-} were all prepared in a similar fashion by addition of a solution of the metal halide or halo anion to a solution containing excess ligand. As our preparative methods for previously reported compounds were different from those originally used, and as the details depend upon the nature of the central metal, complete information is provided for each compound.

Generally, the MoS_4^{2-} complexes were more difficult to prepare in a pure state than their WS_4^{2-} analogues and showed a greater tendency to decompose. The synthesis of $Ni(MoS_4)_2^{2-}$ required rapidity to minimize decomposition, while the Pt(II) complexes required much longer reaction times than their Ni(II) or Pd(II) analogues. The $(C_2H_5)_4N^+$ salts were difficult to recrystallize because of their tendency to form oils. Acidification of the reaction mixture with glacial acetic acid, a technique used by Müller,[7] was found to be beneficial only in the preparation of $Ni(WS_4)_2^{2-}$.

$[(C_3H_7)_4N]_2Ni(MoS_4)_2$. To a solution of 0.238 g (1 mmol) of $NiCl_2 \cdot 6H_2O$ in 15 mL of H_2O was added a solution of 2.0 g of $(C_3H_7)_4NBr$ in 40 mL of CH_3CN. This was added dropwise to a solution of 0.70 g (2.69 mmol) of $(NH_4)_2MoS_4$ in 15 mL of H_2O and 25 mL of CH_3CN. A dark precipitate formed. The reaction mixture was stirred at 0 °C for a few minutes and suction filtered, and the precipitate was washed with 95% ethanol and diethyl ether and dried in vacuo. Best results were obtained when air was excluded and the reaction was performed rapidly; the product could not be successfully recrystallized; yield ca. 90%.

$[(C_3H_7)_4N]_2Ni(WS_4)_2$. To a solution of 0.238 g (1 mmol) of $NiCl_2 \cdot 6H_2O$ in 10 mL of H_2O, was added 10 mL of CH_3CN, and the solution was acidified with several drops of glacial acetic acid. This was added dropwise to a solution of 0.70 g (2.01 mmol) of $(NH_4)_2WS_4$ in 40 mL of 1:3 (v:v) H_2O–CH_3CN. A solution of 2.0 g $(C_3H_7)_4NBr$ in 15 mL of CH_3CN was added dropwise to the resulting solution; precipitation began immediately. The reaction mixture was stirred at 0 °C for 5–10 min and filtered, and the precipitate was washed and dried as described above. The resulting reddish brown solid (crude yield 90%) was recrystallized from CH_3CN.

$[(C_2H_5)_4N]_2Ni(WS_4)_2$. This material was prepared in a fashion similar to that for the tetrapropylammonium salt except that CH_3OH was used instead of CH_3CN. The anion was precipitated by adding a solution of $(C_2H_5)_4NBr$ in 1:1 H_2O–CH_3OH. The yellow-brown solid, obtained in 80% yield, was difficult to recrystallize due to a tendency to oil.

$[(C_3H_7)_4N]_2Pd(MoS_4)_2$. A solution of 0.70 g (2.69 mmol) of $(NH_4)_2MoS_4$ in a mixture of 15 mL of H_2O and 25 mL of CH_3CN was prepared, and a solution of 0.326 g (1.0 mmol) of K_2PdCl_4 in 10 mL of H_2O was added dropwise. The product was precipitated by adding a solution of 2 g of $(C_3H_7)_4NBr$ in 20 mL of 1:1 H_2O–CH_3CN. The deep red product was recrystallized from warm CH_3CN. Yield of crude product was 90%.

$[(C_2H_5)_4N]_2Pd(MoS_4)_2$. This compound was prepared similarly to the previous one but was precipitated by slow (20–30 min) addition of a solution of 2.0 g of $(C_2H_5)_4NBr$ in 20 mL of CH_3OH. The product was recrystallized by dissolution in CH_3CN, addition of CH_3OH until a fine precipitate formed, and cooling at 0 °C for 1–2 days. Dark red irregularly shaped needles were obtained.

$(Ph_4P)_2Pd(MoS_4)_2$. This complex was prepared in a manner similar to that for the $(C_2H_5)_4N^+$ salt but was precipitated by the dropwise addition of a solution of 1 g of Ph_4PBr in 30 mL of CH_3CN. The brick red product (80% yield) was recrystallized from nitromethane. Anal. Calcd for $C_{48}H_{40}P_2S_8Mo_2Pd$: C, 46.76; H, 3.29; P, 5.02; S, 20.79; Mo, 15.55; Pd, 8.62. Found: C, 46.23; H, 3.57; P, 5.29; S, 20.03; Mo, 14.32; Pd, 8.93.

$[(C_2H_5)_4N]_2Pd(WS_4)_2$. A solution of 0.326 g (1.0 mmol) of K_2PdCl_4 in 10 mL of H_2O was added dropwise over a 10-min period to a stirred solution of 0.70 g (2.01 mmol) of $(NH_4)_2WS_4$ in 10 mL of H_2O and 30 mL of CH_3CN. The reaction product was precipitated with a solution of 2.0 g of $(C_2H_5)_4NBr$ in 10 mL of H_2O and 10 mL of CH_3CN. The rust colored product (85% yield) could be recrystallized from either CH_3NO_2 or CH_3CN by cooling concentrated solutions at 0 °C for several days. Anal. Calcd for $C_{16}H_{40}N_2S_8W_2Pd$: C, 19.39; H, 4.07; N, 2.85; S, 25.88; W, 37.10; Pd, 10.74. Found: C, 19.68; H, 4.08; N, 3.02; S, 25.57; W, 36.82; Pd, 11.04.

$[(C_3H_7)_4N]_2Pt(MoS_4)_2$. A procedure similar to the one described above was employed, except that 0.70 g (2.7 mmol) of $(NH_4)_2MoS_4$ in 15 mL of H_2O and 25 mL of CH_3CN was used, the reaction was stirred for 4–8 h, and the solution did not need to be filtered before addition of a solution of 2.0 g of $(C_3H_7)_4NBr$ in 10 mL of H_2O. The dark red product, obtained in 75% yield, was recrystallized from CH_3CN. Anal. Calcd for $C_{24}H_{56}N_2S_8Mo_2Pt$: C, 28.47; H, 5.58; N, 2.77; S, 25.35; Mo, 18.96; Pt, 19.28. Found: C, 27.77; H, 5.37; N, 3.02; S, 25.03; Mo, 18.65; Pt, 18.74.

$[(C_2H_5)_4N]_2Pt(MoS_4)_2$. This preparation was similar to the one above except that precipitation of the crude product was accomplished by addition of a solution of 2.0 g of $(C_2H_5)_4NBr$ in 20 mL of CH_3OH. The product was obtained in 65% yield.

$[(C_2H_5)_4N]_2Pt(WS_4)_2$. A solution of 0.415 g (1.0 mmol) of K_2PtCl_4 in 10 mL of H_2O and 10 mL of CH_3CN was added to a solution of 0.70 g (2.01 mmol) of $(NH_4)_2WS_4$ in 40 mL of H_2O and 40 mL of CH_3CN. The reaction mixture was stirred at room temperature for 8–12 h and filtered to remove a small amount of yellow precipitate which had formed. The product was precipitated by addition of a solution of 2.0 g of $(C_2H_5)_4NBr$ in 20 mL of H_2O. A red product was obtained in yields of 50–70% and was recrystallized from warm CH_3CN. Well-formed, nearly cubic crystals were obtained on slow cooling. Anal. Calcd for $C_{16}H_{40}N_2S_8W_2Pt$: C, 17.80; H, 3.73; N, 2.59; S, 23.75; W, 34.05; Pt, 18.06. Found: C, 18.76; H, 3.89; N, 2.99; S, 24.28; W, 32.10; Pt, 17.70.

Acknowledgment. We thank Mr. David E. Hansen for the rapid-scan cyclic voltammograms and Professor P. H. Rieger for several informative discussions and experimental assistance. This research was supported in part by the Research Corp. and by the Brown University Materials Research Laboratory, to whom we express our thanks.

Registry No. $[(C_3H_7)_4N]_2Ni(MoS_4)_2$, 73952-49-5; $[(C_3H_7)_4N]_2Ni(WS_4)_2$, 73952-50-8; $[(C_2H_5)_4N]_2Ni(WS_4)_2$, 73952-51-9; $[(C_3H_7)_4N]_2Pd(MoS_4)_2$, 73952-52-0; $[(C_2H_5)_4N]_2Pd(MoS_4)_2$, 73952-53-1; $(Ph_4P)_2Pd(MoS_4)_2$, 74006-31-8; $[(C_2H_5)_4N]_2Pd(WS_4)_2$, 74006-32-9; $[(C_3H_7)_4N]_2Pt(MoS_4)_2$, 74006-33-0; $[(C_2H_5)_4N]_2Pt(MoS_4)_2$, 74006-34-1; $[(C_2H_5)_4N]_2Pt(WS_4)_2$, 73952-54-2; $Ni(MoS_4)_2^{3-}$, 73926-35-9; $Ni(WS_4)_2^{3-}$, 73926-36-0; $Ni(MoS_4)_2^{4-}$, 73926-37-1; $Ni(WS_4)_2^{4-}$, 73926-38-2; $Pd(MoS_4)_2^{3-}$, 73926-39-3; $Pd(WS_4)_2^{3-}$, 73926-40-6; $Pd(MoS_4)_2^{4-}$, 73926-41-7; $Pd(WS_4)_2^{4-}$, 73926-42-8.